EXTRACTION AND CHARACTERIZATION OF NANOCELLULOSE FROM MAHANG WOOD

by

NOOR SAHIRAH BINTI MUHAZELI

A report submitted in partial fulfillment of the requirements for the degree of Bachelor of Applied Science (Materials Technology) with Honours

FACULTY OF EARTH SCIENCE
UNIVERSITI MALAYSIA KELANTAN

2017

DECLARATION

I declare that this thesis entitled “Extraction and Characterization of Nanocellulose from Mahang Wood” is the result of my own research except as cited in the references. The thesis has not been accepted for any degree and is not concurrently submitted in candidature of any other degree.

Signature :_____

Name : _____

Date : _____

ACKNOWLEDGEMENT

Final Year Project (FYP) is a very good opportunity for me to do my own research and writing my own thesis. Furthermore, this is a single step for me to go on with my journey to adapt myself in developing me to become a good student with plenty of experiences and knowledge. I am very grateful to the University Malaysia Kelantan (UMK) and the Faculty of Earth Science (FSB) for establishing a Final Year Project (FYP) to all of the students. The cooperation and contributions in providing useful information during the progress of the research have been an immense help.

Besides, my heart full of thanks also goes to Dr. Asanah Binti Radhi who is my supervisor for FYP. Under her continuous guidance that always spends her time in guiding, advising, giving comment and providing a lot of valuable information in preparing this project, I was able to finish up all of my FYP successfully. It was such a good experience by working with Dr. Asanah, who is one of the lecturers that are well respected in University Malaysia Kelantan. Even though she is busy with her schedule, her willingness to assist me in accomplishing this Final Year Project has been a precious and great value.

Furthermore, my fellow undergraduate students, my fondest family, friends and also the lab assistants should also be recognized for their support. All this while, they gave me help, guidance, moral support and courage in completing this task. I might not be able to repay their kindness but I may pray for their blessing in life. Last but not least, I would like to thanks to all that help me directly or indirectly in finishing my Final Year Project. Thank you very much.

EXTRACTION AND CHARACTERIZATION OF NANOCELLULOSE FROM MAHANG WOOD

ABSTRACT

In this study, an improved approach for production and characterization of regenerated celluloses from mahang wood is proposed. The purpose of this research is to extract cellulose from mahang (*Macaranga gigantea*) wood and convert the extracted cellulose (MCC) to nanocellulose using ionic liquid pretreatment. 1-butyl-3-methylimidazolium chloride (BMIMCl) was used to treat cellulose that has been extracted from mahang wood. Three different regenerated celluloses were obtained from the different weight ratio of celluloses treated with BMIMCl (2 wt %, 5 wt % and 8 wt %). X-ray diffraction (XRD), Fourier transform infrared analysis (FTIR), field emission-scanning electron microscopy (FESEM), and thermogravimetric analysis (TGA) were used to characterize the structural, morphological and thermal properties of celluloses and also the regenerated celluloses samples. The results of characterizations indicated that 2 wt % of regenerated celluloses with the highest amount of ionic liquid used obtained high crystallinity compared to 5 wt % and 8 wt % regenerated celluloses. Hence, from all of the characterizations of regenerated celluloses, only 2 wt % regenerated celluloses can be correlate to the real properties and characteristics of nanocellulose (NCCs).

PENGESKTRAKAN DAN PENCIRIAN NANO SELULOSA DARI KAYU MAHANG

ABSTRAK

Di dalam tesis ini, dibentangkan satu pendekatan yang lebih baik untuk pengekstrakan dan pencirian selulosa yang dijana dari kayu mahang. Tujuan kajian ini adalah untuk mengekstrak selulosa daripada kayu mahang (*Macaranga gigantea*) dan menukar selulosa ekstrak (*MCC*) kepada nano selulosa (*NCCs*) dengan menggunakan cecair ion.1-butil-3-methylimidazolium klorida (*BMIMCl*) telah digunakan untuk merawat selulosa yang telah diekstrak daripada kayu Mahang. Tiga jenis selulosa terjana semula telah diperolehi daripada perbezaan nisbah peratus berat kering yang dirawat dengan *BMIMCl* (2 wt %, 5 wt % dan 8 wt %). Belau sinar-x (*XRD*), spektroskopi inframerah transformasi Fourier (*FTIR*), paparan emisi mikroskopi elektron penskanan (*FESEM*), dan analisis termogravimetri (*TGA*) telah digunakan untuk mencirikan selulosa sampel dan juga selulosa terjana semula dari segi struktur, morfologi dan sifat terma. Keputusan pencirian menunjukkan bahawa, 2 wt % peratus berat kering selulosa terjana semula mencatatkan tahap kehabluran tinggi dengan penggunaan jumlah cecair ion yang tertinggi berbanding dengan 5 wt % dan 8 wt % berat kering. Oleh yang demikian, daripada semua pencirian selulosa terjana semula, hanya 2 wt % peratus berat kering selulosa terjana semula menghubungkaitkan kepada ciri dan sifat sebenar nano selulosa (*NCCs*).

TABLE OF CONTENTS

		PAGE
DECLARATION		**i**
ACKNOWLEDGEMENT		**ii**
ABSTRACT		**iii**
ABSTRAK		**iv**
TABLE OF CONTENT		**v**
LIST OF TABLES		**vii**
LIST OF FIGURES		**viii**
LIST OF ABBREVATIONS		**x**
LIST OF SYMBOLS		**xi**
LIST OF APPENDICES		xii
CHAPTER 1 INTRODUCTION		
1.1	Background of Study	1
1.2	Problem Statement	3
1.3	Objectives	3
1.4	Significance of Study	4
CHAPTER 2 LITERATURE REVIEW		
2.1	Mahang (*Macaranga spp.*)	5
2.2	Cellulose (MCC)	6
2.3	Hemicellulose	7
2.4	Lignin	8
2.5	Nanocellulose (NCCs)	9
2.6	Extraction and isolation of cellulose	10
2.7	Ionic liquid (IL)	11
CHAPTER 3 MATERIALS AND METHOD		
3.1	**Methodology**	
	3.1.1 Sample preparation	14
	3.1.2 Cellulose extraction	15
	(a) Extraction of free extractives	15

(b) Holocellulose 16
(c) Alpha cellulose 18
3.1.3 Nanocellulose production 19
3.2 Characterization of nanocellulose
3.2.1 X-ray diffraction (XRD) 21
3.2.2 Fourier transform infrared analysis (FTIR) 22
3.2.3 Field emission-scanning electron microscopy (FESEM) 22
3.2.4 Thermogravimetric analysis (TGA) 22
RESEARCH FLOWCHART 23
CHAPTER 4 RESULT AND DISCUSSION
4.1 X-ray diffraction (XRD) analysis 24
4.2 Fourier transform infrared (FTIR) analysis 29
4.3 Field emission-scanning electron microscopy (FESEM) analysis 32
4.4 Thermogravimetric analysis (TGA) analysis 35
CHAPTER 5 CONCLUSIONAND RECOMMENDATIONS 39
REFERENCES 41
APPENDICES 44

LIST OF TABLES

NO	TITLE	PAGE
3.1	Total amount of cellulose and IL in different wt % of regenerated celluloses, NCCs.	19
4.1	The crystallinity (Crl) and crystallite size of MMC and regenerated celluloses prepared with different weight ratio (2 wt %, 5 wt % and 8 wt%).	28
4.2	Group frequency of absorption bands of cellulosic samples.	31

LIST OF FIGURES

NO	TITLE	PAGE
2.1	Chemical structure of cellulose.	6
2.2	Structure of xylan.	8
2.3	Major structural unit of lignin	9
2.4	The structure of 1-butyl-3-methylimidazolium chloride (BMIMCl)	13
3.1	Mahang wood that was cut and chopped	14
3.2	Extraction process of mahang powder	15
3.3	Vacuum drying of excess solvents	16
3.4	Production of holocellulose	17
3.5	Production of alpha cellulose	18
3.6	2 wt %, 5 wt% and 8 wt% of regenerated celluloses production	19
3.7	Regenerated cellulose (NCCs) obtained after freeze dry	20
4.1	XRD pattern of Cellulose pure MMC (a), alpha cellulose (b) and regenerated celluloses treated with an ionic liquid at 2 wt% (c), 5 wt % (d) and 8 wt% (e).	25
4.2	XRD pattern of 2 wt % regenerated celluloses, NCCs.	26
4.3	FTIR Spectra of Cellulose pure MMC (a), alpha cellulose (b) and regenerated celluloses treated with an ionic liquid at 2 wt% (c), 5 wt % (d) and 8 wt % (e)	29
4.4	(a): Structure and appearance of 2 wt % regenerated cellulose fiber by FESEM at high magnification (×15000).	32
	(b): Structure and appearance of 2 wt % regenerated cellulose fiber by FESEM at low magnification (×800).	33
	(c): Structure and appearance of 2 wt % regenerated cellulose fiber by FESEM at low magnification (×500).	33
	(d): Structure and appearance of 2 wt % regenerated cellulose fiber by FESEM at very low magnification (×60).	34
4.5	(a): TG curves for cellulose pure (MMC) (a), alpha cellulose (b) and at	35

2 wt% (c),5 wt % (d) and 8 wt % (e) of regenerated celluloses.
(b): DTG curves for cellulose pure (MMC) (a), alpha cellulose (b) and 37
at 2 wt% (c),5 wt % (d) and 8 wt % (e) of regenerated celluloses.

LIST OFABBREVIATIONS

MFC	Microfibrillated cellulose
MCC	Micro crystalline cellulose
NCCs	Nano crystalline cellulose
BNC	Bacterial nanocellulose
IL	Ionic liquid
AMIMCl	1-allyl-3-methylimidazolium-chloride
EMIMAc	1-ethyl-3-methylimidazolium-acetate
BMIMCl	1-butyl-3-methylimidazolium chloride
EMIMDEP	1-ethyl-3-methyl imidazolium diethyl phosphate
BMIMCL	1-butyl-3-methylimidazolium chloride
XRD	X-ray diffraction
FTIR	Fourier transform infrared analysis
FESEM	Field emission-scanning electron microscopy
TGA	Thermogravimetric analysis
DTG	Differential thermogravimetric

LIST OF SYMBOLS

β	Beta, FWHM
N	Normality
λ	Lambda
θ	Theta
Å	Angstrom unit
$V\rho$	Density variation
T_{max}	Maximum temperature
I_{002}	Peak intensity corresponding to crystalline
I_{am}	Peak intensity of the amorphous fraction
w	Crystallite size
Crl	Crystallinity index
wt %	Weight percentage

LIST OF APPENDICES

A 1: Mahang powder
A 2: Extraction samples after oven dry
A 3: Holocellulose sample after oven dry
A 4: Alpha cellulose obtained after oven dry
A 5: Completed regenerated celluloses production
A 6: Separation process of ionic liquid

CHAPTER 1

INTRODUCTION

1.1 Background of Study

The developments in materials science and nanotechnology today recently provide the expertise to the production of advance materials from biological resources. Hence, the identification and exploitation of this knowledge should enable the sustainable conversion of forest-based raw materials such as wood into innovative materials.

Wood is one of the most useful and attractive bio-based materials that gain interests in materials science especially in biocomposite production (Dufresne, 2013). It has widely used because of a wide range of application and also its complex and extraordinary structure. The contents of cellulose in wood are approximately 40-50 wt% cellulose, which are half in nanocrystalline form and half in amorphous form (Dufresne, 2013). Besides, wood has many attractive properties such as it has low density, low thermal expansion, renewable and also desirable mechanical strength (Pandey, 1999). There are a few types of wood such as hardwood, softwood and also nonwood. Hardwood (angiosperms) refers to the broad leaf trees and dark in colour, for examples, oak and Mahang (*Macaranga spp.*). Softwoods (gymnosperms) refer to the narrow leaf trees and lighter in colour, for examples an oil palm (Pandey, 1999).

Generally, the main compositions of the lignocellulosic biomass consist of three biopolymers: cellulose (~30-50 % by weight), hemicelluloses (~19-45 % by weight) and

lignin (~15-35 % by weight) (Bee et al., 2015). Cellulose, hemicelluloses, and lignin with a ratio of 4:3:3 in the cell walls may differ if it were extracted from various sources such as hardwood, softwood, and non-wood (Bee et al., 2015). From the ratio, it is clearly shown that cellulose has the highest number of the ratio in the plant cell walls compared to hemicelluloses and lignin. This is because cellulose is one of the most important components that determine the structures and strength in the cell wall of wood fiber (Gardner et al., 1974).

Cellulose is one of the most abundant biomaterials that are very useful and can be obtained from numerous sources on earth. Plus, cellulose also can be used as starting materials for nanocellulose production via various process, includes strong acid hydrolysis and treatment of cellulose with Ionic Liquid (IL). Acid hydrolysis will introduce the negative charges from the acidic substances to the structure of native cellulose and it will hydrolyse the amorphous part into the nanosized fiber (Mat Zain, 2014). Besides, dissolution of cellulose with IL also allows the utilization of cellulose by combined the environmentally preferable solvents and bio-renewable feed-stocks that considered as major green chemistry principle (Zhu et al., 2006).

Moreover, nanocellulose is one of the natural materials in a nanoscale dimension that has been used especially in making of the nanocomposite. Other than that, nanocellulose has various unique properties such as renewable materials, availability, unique morphology, lightweight and low cost (Habibi et al., 2009). The applications of nanocellulose include as reinforcing agents in nanocomposites, biodegradable films, barriers for packaging, additives in foods, texturing agents in cosmetics and also in medical devices (Mohammad et al., 2014).

1.2 Problem statement

In the wood production of products such as the manufacturing of the furniture, there are abundant of wood residues such as the small and undesirable parts of wood that will probably be throw away after the production of furniture is completed. Therefore, this study was one of the solutions where the abundant of wood residues can be fully utilized in most beneficial ways. Besides, the type of wood that has been used in this study that is mahang (*Macaranga sp*) is one of under-utilized wood types and considered as one of the types of wood that does not often used in wood industry but have the great potential to serve as the timber supply alternative to the industry woods if their properties improved (Ang et al., 2014). Hence, by extracting the cellulose from this type of wood and convert to nanocellulose, it can absolutely improve its variety of application in the industry such as in timber industry, automotive industry, interior applications, constructions, electronics, cosmetics, packaging and also biomedicine (Klemm et al., 2011). Thus, it is shown that there is a huge potential and most effective method if the wood can be fully utilized in this beneficial ways.

1.3 Objectives

The objectives of this study are as followings:

1. To extract cellulose from Mahang (*Macaranga gigantea*) wood.
2. To convert cellulose (MCC) to nanocellulose (NCCs) using an ionic liquid as a pretreatments solvent.
3. To characterize nanocellulose (NCCs) extracted from Mahang (*Macaranga gigantea*) wood.

1.4 Significance of Study

Cellulose (MCC) that has been extracted was converted to a nanoscale dimension that is the regenerated celluloses or nanocellulose (NCCs). From the extraction of cellulose, the properties were characterized and it enhanced the specific properties needed for nanocellulose applications such as in nanocomposites. Besides, apart from conventional uses of mahang wood such as veneer and plywood, this study was progressing to determine the uses and efficiency of hardwood types in nanocomposite applications. Therefore, the utilization of nanocellulose from mahang wood had definitely opened up new avenues for our natural resources. Currently, there were none of the isolation processes of nanocellulose using mahang (*Macaranga gigantea*) was reported. Hence, this study was one of the new studies about the extraction and characterization of regenerated celluloses (NCCs) from Mahang (*Macaranga gigantea*) wood.

CHAPTER 2

LITERATURE REVIEW

2.1 Mahang (*Macaranga spp.*)

Mahang (*Macaranga spp.*) is a pioneer and soft-wooded tree species that consider as light density wood types and have abundant quantity in the logged-over forest in Southeast Asia (Ang et al., 2009). The populations are generally found in village-thickets, wastelands, at the edge of forest reserves or in swampy forests (Zakaria et al., 2008). In Malaysia, there are only 27 species of mahang (*Macaranga spp.*) from the total of 280 species worldwide (Zakaria et al., 2008). Hence, mahang is currently not abundance and commercially available at the moment in Malaysia, but it can be commercialized due to their fast-growing ability. Plus, mahang also is an evergreen tree that can reach a height of 20 m (Zakaria et al., 2008). Besides that, mahang also has the great advantages such as exotic colours and texture, cheaper price and also abundance availability.

From the other sides, mahang is still under-utilized plants due to it poor properties and the information regarding the species is also limited, but it can greatly contribute the great potential in nanocomposite (NCCs) production by added value into the wood types (Noor Azrieda et al., 2012). Apart from that, the disadvantages of mahang (*Macaranga spp.*) such as dimensional stability, inferior mechanical strength, and low durability also can be improved (Ang et al., 2014). For instance, the percentage of cellulose in mahang wood has been studied in this research for the extraction of nanocellulose (NCCs) using

ionic liquid (IL) for nanocomposite applications has proved that mahang can be improved in this beneficial ways. Thus, it is clearly shown that mahang (*Macaranga spp.*) is one of the wood types that can use and greatly improve its applications wider in industry.

2.2 Cellulose

Cellulose is abundantly found on earth especially in wood and other lignocellulosic biomass. The term of cellulose can define as Microcrystalline cellulose (MCCs) which is in microsize forms. Plus, cellulose also is one of the examples of natural polymers and almost inexhaustible raw materials that act as a key source of sustainable materials on an industrial scale. In general, cellulose also considers as a fibrous, tough, water-insoluble substances that important in determining the structure of plant cell walls (Habibi et al., 2009).

Chemically, cellulose considered as a long chain polymer with repeating units of anhydroglucose units linked by β-glycosidic bonds at the one and four carbon atoms containing both crystalline and amorphous region and represented by generic formula $(C_6H_{10}O_5)_n$ (Gardner et al., 1974).

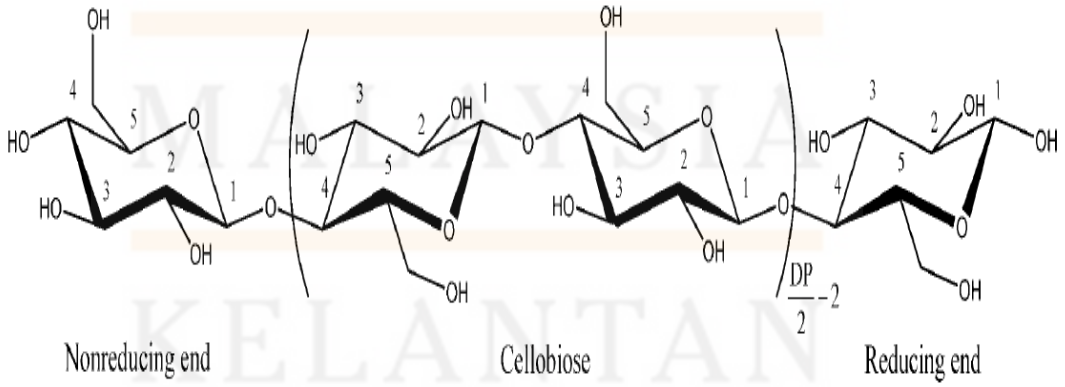

Figure 2.1: Chemical structure of cellulose.

Generally, cellulose in wood, both hardwood and softwood have percentages between 40 % to 47 %, which content in hardwood is higher than in softwood (Hwa et al., 2009). Besides, cellulose also is a semi-flexible polymer which its stiffness and rigidity of the molecules are mainly due to the intramolecular hydrogen bonding. Hence, the property is reflected due to its high viscosity in solution, a high tendency to crystallize and its ability to form fibrillar strands (Granström et al., 2009).

Besides, cellulose also is a relatively stable polymer according to the hydrogen network that does not dissolve in common aqueous solvents (Frone, Panaitescu, & Donescu, 2011). In most conditions, cellulose is often surrounded by hemicelluloses (dry matter accounting for 20-35 %) and lignin (dry matter accounting for 5-30 %) (Chen.Hz, 2014). Furthermore, cellulose also is the main component of various natural fibers such as cotton, flax, hemp, jute and sisal (Moran et al., 2008). Generally, cellulose represents about one-third of plant tissues and it can be restocked by photosynthesis. There are several types of cellulose includes I, II, III, IV and V. Type I cellulose showing better mechanical properties (Moran et al., 2008).

2.3 Hemicellulose

Hemicellulose is defined as the polysaccharide that easily separated from plant tissue that considers as semi-finished products of cellulose or precursor molecules of cellulose (Chen.Hz, 2014). Other than that, hemicellulose is one of the main components in the plant fiber materials. The purification of hemicellulose was conducted referring to the different alkaline solubilities with hemicellulose.

Hence, according to Whistler (1978), hemicellulose is the polysaccharide that extracted by an alkaline solution, except cellulose and pectin (Chen.Hz, 2014). Plus, hemicellulose is also a copolymer that composed of different amounts of several saccharide molecules unlike cellulose (Chen.Hz, 2014). In wood, the main hemicellulose is a xylan which is more specifically is an *O*-acetyl-4-*O*-methylglucurono-β-D-xylan (Figure 2.2) (Laine, 2005).

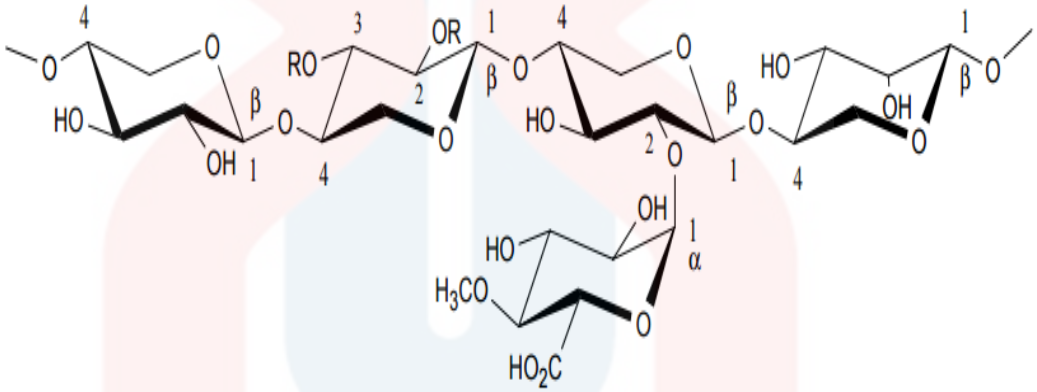

Figure 2.2: Structure of xylan (Laine, 2005).

2.4 Lignin

Lignin also is one of the most abundant organic polymers in plants. Generally, the content of lignin in wood is 20-40 % (Chen.Hz, 2014). Besides, lignin also considers as a complex polymer that composed of complicated phenyl propane units that are nonlinearly and randomly linked. Lignin is derived from renewable resources such as grasses, trees, and agricultural crops. Plus, lignin constituent is about 30% in wood. Furthermore, lignin also considers as a nontoxic and extremely versatile in their performance. Lignin has become the production of by-products of pulping process in the world over 30 million tons per year (Jung et al., 2012).

The three major structure of lignin, and 4-hydroxyphenyl (1), guaiacyl (2), and syringyl (3) structures are conjugated in order to produce a three-dimensional lignin polymer (Jung et al., 2012). Figure 2.3 shows the three main monomers that consider as the major structural unit of lignin.

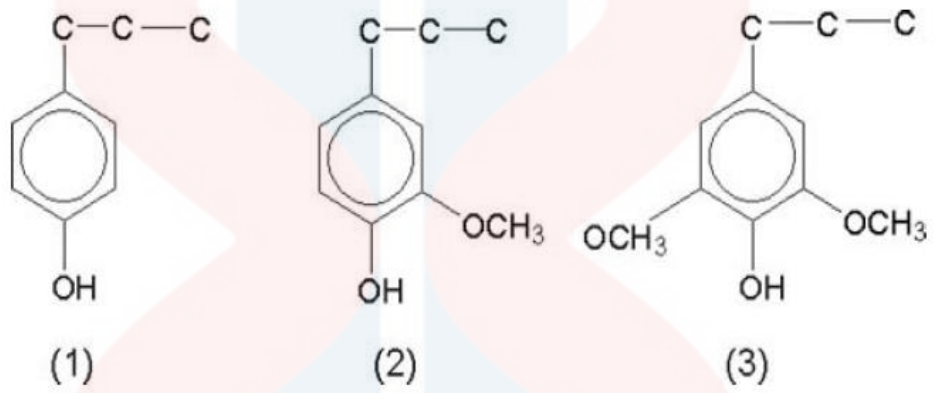

Figure 2.3: Major structural unit of lignin, 4-hydroxyphenyl (1), guaiacyl (2), and syringyl (3) structures (Jung et al., 2012).

2.5 Nanocellulose (NCCs)

Nanocellulose or nanocrystalline cellulose (NCCs) is one of the natural materials in a nanoscale dimension that has the diameter less than 100 nm and length varies from 100 nm to several micrometers (Ma et al., 2015). Besides, NCCs also refers to the regenerated cellulose. The term 'nanocellulose' was overcome from the result of isolation process from various types of plant resources.

Moreover, nanocellulose can also be produced from various resources such as plant biomass, algae and a sea animal (tunicate) (Lee et al., 2014). There are various sources of nanocellulose that can be obtained from plant biomass such as from hemp, sugarcane bagasse, sisal, cotton and bacterial (Ma et al., 2015). Nanocellulose (NCCs) which obtains from cellulose (MCC) is actually creating a revolution in biobased materials for

a variety of applications (Bee et al., 2015).

The benefits of NCCs includes a nanoscale dimension, high surface area, unique optical properties, high crystallinity, biodegradable, renewable resources and high specific modulus and strength (Soni et al., 2015). Hence, this benefits leads to the production of a precious green alternative to materials, construction, automobile, packaging, transportation and biomedical fields (Bee et al., 2015). There are several types of nanocellulose includes microfibrillated cellulose (MFC), nanocrystalline cellulose (NCC) and bacterial nanocellulose (BNC) (Mohammad et al., 2014). The great potential of NCCs has been demonstrated for special functional nanomaterials, but it is categorizing as a biobased reinforcing nanofiller as nanomaterials have attracted significant interest over the past 20 years. Moreover, cellulose nanoparticles have a strong tendency for self-association because of the omnipresence of interacting surface hydroxyl. Apart from that, the main challenge with nanoparticles is related to their homogeneous dispersion within a polymeric matrix (Dufresne, 2013).

2.6 Extraction and isolation of cellulose

There are many sources of cellulose that can be isolated and extracted from various types of plants. Current studies indicate the possibility to obtain natural cellulose fibres (MMC) from plants such as cotton linter, wheat straw, rice straw, corn stalks, husk leaves, stalks of sorghum pineapple leaves, banana leaves, sugar cane and even nettle (Kopania et al., 2012). Waste materials also can be used to obtain the cellulose fibers in the production or isolation of microcellulose (MCC) or nanocellulose (NCCs) fibers.

Cotton linter is one of the abundant resources of cellulose that has greatly potential to be used in the production of hydrophilic nanocomposites (Morais et al., 2013). Furthermore, extraction of nanocellulose from raw cotton linter also does not require pulping. The total of cotton linter produces worldwide is around 2.5 million metrics tons, which 42 million metric ton of cotton lint produced in 2010 (Morais et al., 2013).

Other than that, there are several methods to extract and isolate the nanocellulose (NCCs) includes mechanical, chemical and enzymatic method. Acid hydrolysis was generally performed to remove the amorphous region to obtain high crystalline particle. Hydrochloric acid (HCl) and sulphuric acid (H_2SO_4) were the high concentration of acid that used in acid hydrolysis process. Refined fibers with several micrometers long can be produced by the mechanical method (Ma et al, 2015). Besides that, alkaline hydrolysis also can be performed to determine the partial separation of the cellulose fibers from the cell wall. This alkaline hydrolysis is usually carried out using diluted solutions of NaOH (1-10 %) at low or high temperatures and also concentrated NaOH solutions over 10 % only at low temperatures (Frone et al., 2011).

2.7 Ionic liquid

Recently, ionic liquid has been used widely as the new type of green solvent pretreatments used in various areas of research and industrial of applications. Ionic liquids are defined as the organic salts that comprise of ions (cations or anions) with low melting temperature (<100˚). Plus, ionic liquids also considered as green solvents that contain formate, anions of chloride, acetate or alkyl phosphonate anion (Tan et al.,

2011). Plus, an ionic liquid (IL) also considered as green solvents due to the properties of lower vapour pressure and decreased the risk of environmental damage.

Ionic liquid pretreatments can reduce the crystallinity of cellulose and partially remove hemicellulose and lignin while not generating degradation products which are inhibitory to enzymes or fermenting microorganisms. Pretreatment with IL is less energy demanding, easier to handle and more environmentally friendly than other pretreatment methods such as mechanical milling, steam explosion, acid, base, or organic solvent processes. Tan et al (2011) proved that ionic liquids can dissolve cellulose and have great versatility in the field of cellulose technology. By the addition of water, ethanol or acetone, cellulose can be easily generated from its ionic liquid solutions (Frone et al., 2011).

Plus, ionic liquid solvents can be recovered and reused after its regeneration. This liquid can be recovered by many methods such as evaporation, ion exchange and reverse osmosis (Frone et al., 2011). Ionic liquid also has been used because of the unique physiochemical properties and its potential to be an environmentally friendly (Tan et al, 2015). These liquids also are extremely low vapour pressure, chemically and thermally stable and also present inflammable (Frone et al., 2011).

Moreover, there are many types of ionic liquids that have been used as media for dissolving cellulose from lignocellulosic biomass in the pretreatments method such as 1-allyl-3-methylimidazolium-chloride (AMIMCl), 1-ethyl-3-methylimidazolium-acetate (EMIMAc),1-butyl-3-methylimidazolium chloride (BMIMCl) and 1-ethyl-3-methyl imidazolium diethyl phosphate (EMIMDEP) (Tan et al., 2011). In this study, BMIMCl is used to dissolve the cellulose. BMIMCl considers as the solution that has high chloride concentration and the activity in BMIMCl was assumed to have highly effective

in breaking the hydrogen bonding network that present in the cellulose. Hence, if the BMIMCl present in the water, the solubility of cellulose through competitive hydrogen bonding will decrease (Zhu et al., 2006). Figure 2.4 shows the structure of BMIMCl.

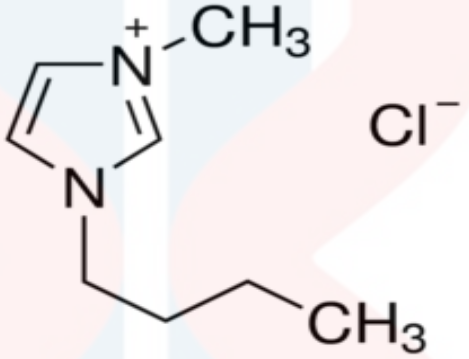

Figure 2.4: The structure of 1-butyl-3-methylimidazolium chloride (BMIMCl).

CHAPTER 3

MATERIALS AND METHODS

3.1 Methodology

3.1.1 Sample preparation

Sample preparation of the wood fibers required multiple steps. First of all, the mahang wood was cut and chopped to the smaller size as shown in Figure 3.1. Then, the fibers of mahang wood were ground in order to change the wood fibers into powder. Next, the wood powder was passing through a 250-micron stainless steel sieve and it was dried overnight in an oven at 100 ˚C. Finally, mahang powder was obtained in desired amount and size.

Figure 3.1: Mahang wood that was cut and chopped.

3.1.2 Cellulose extraction

(a) Extraction of extractives

According to the TAPPI test method T204, the extractives (dewaxing) was removed by using Soxhlet apparatus (Oksman et al., 2011). Approximately 10 g of powder samples was used in this extraction. First of all, the Soxhlet apparatus was set up. Then, the sample has been extracted for 6 hours at 150 ˚C using a mixture of ethanol and toluene in the ratio of 2:1 (Figure 3.2). After 6 h, the process has been stopped and the sample was allowed to cool to room temperature.

Figure 3.2: Extraction process of mahang powder.

The sample then was placed in Buckner funnel and vacuum drying at room temperature to remove the excess solvents (*see* Figure 3.3). After drying, the sample was re-extracted and ethanol was used to remove trace of toluene. Then, the sample was dried by using vacuum for 24 h to remove the traces of residual solvents (Oksman et al., 2011) (Oksman et al., 2011). The free extractives were collected in the extraction timble that have been inserted to Soxhlet apparatus and the extractives were collected in the round bottles.

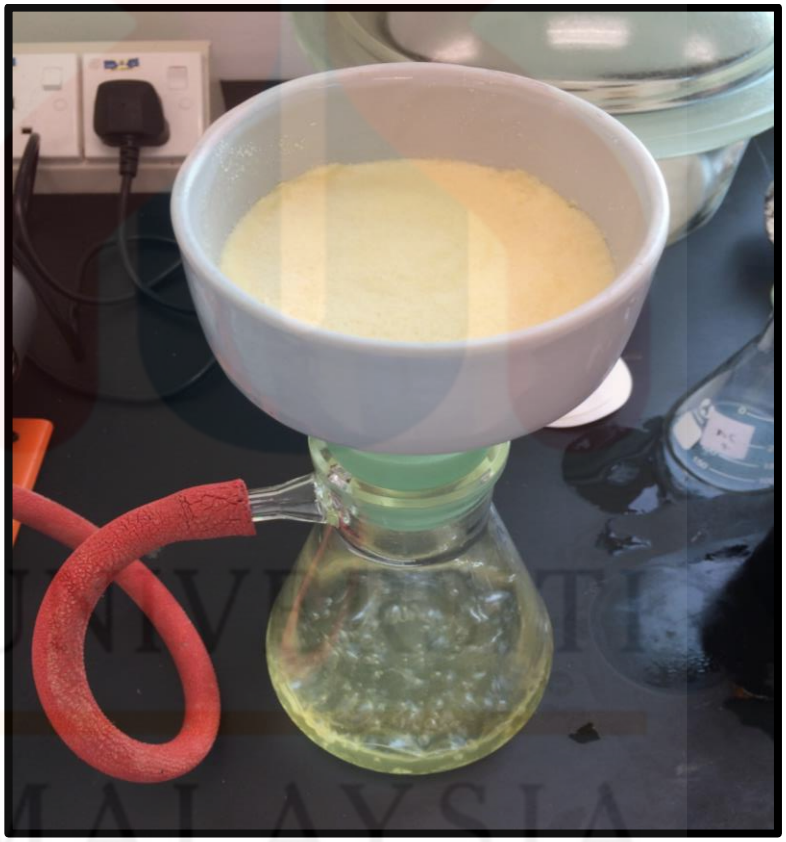

Figure 3.3: Vacuum drying of excess solvents.

(b) Holocellulose

In order to bleach the extractive-free bio-residue, the sample of free extractives was weighed until achieved desired weight that was 5 g (Oksman et al., 2011). Then, 5 g sample was placed in a conical flask containing 100 ml distilled water, 5 ml of 10 %

acetic acid (CH_3COOH) and 1.5 g of sodium chlorite ($NaClO_2$). The mixtures were heated and the temperature was maintained at 70 ˚C for 4 h continuous process as shown in Figure 3.4.

During 4 h, four further additions of 5 ml of 10 % CH_3COOH and 1.5 g $NaClO_2$ was carried out at every 30 minutes until the bleaching was completed. Then, the conical flask was placed in ice to be cooled. The samples must be washed with cold distilled water and 25 ml of acetone before it would be filtered. Then, the samples were filtered by using the filtering flash and sapped by the vacuum pump. After finished the step, the sample was oven dried at 50 ˚ C for 24 hours. After 24 h, the hollocellulose was obtained by weighing the sample.

Figure 3.4: Production of holocellulose

(c) Alpha cellulose

In order to extract alpha cellulose that has been obtained from the hollocellulose production process, 2 g of hollocellulose and 15 ml of 17.5 % NaOH were placed in a conical flask. After 1 minute of continuos stirring, 10 ml of 17.5 % NaOH was added and it has been stirred in 45 s. Then, 10 ml of 17.5 % NaOH was added and it was stirred for 3 minutes.

Figure 3.5: Production of alpha cellulose.

After that, four further additions of 10 ml of 17.5 % NaOH was added at every 2.5 minutes during 10 minutes. The conical flask was closed and it was left for 30 minutes. After 30 minutes, 100 ml of distilled water was added and it was left again for 30 minutes to allow continuous stirring. After 1 hour, the samples have been filtered and

washed by using 8.3 % of NaOH and cold distilled water. The samples were soaked in 2 N of CH_3COOH and it were filtered and oven dried at 50 ˚C for 24 h. Lastly, cellulose was finally obtained and extracted. Figure 3.5 showed the production process of alpha cellulose.

3.1.3 Nanocellulose production

Nanocellulose (NCCs) was prepared by using ionic liquid (IL) as the solvent of the pretreatments. Firstly, 2 wt %, 5 wt % and 8 wt % of extracted cellulose were dissolved in 1-butyl-3-methylimidazolium chloride (BMIMCl) ionic liquid with vigorous stirring (*see* Figure 3.6). For each total amount of weight percentage, different ratio amount of extracted cellulose and ionic liquid were added as tabulated in Table 3.1.

Table 3.1 shows the total amount of cellulose and IL in different 2 wt %, 5 wt % and 8 wt % of regenerated celluloses

wt % of regenerated cellulose, NCCs	Total amount (cellulose)	Total amount (IL)
2 wt %	2.0 g	98.0 g
5 wt %	2.5 g	47.5 g
8 wt %	4.0 g	46.0 g

The heterogeneous mixture was heated at 90 ˚C for 12 hours on a magnetic hot plate stirrer. After 12 hours, 3 of the different wt % samples were washed with the distilled water until the ionic liquid fully separated. Then, the precipitates were freeze dried for 24 hours. Last but not least, the regenerated celluloses (NCCs) for 3 different wt % obtained as shown in Figure 3.7 and it was kept for the characterization process.

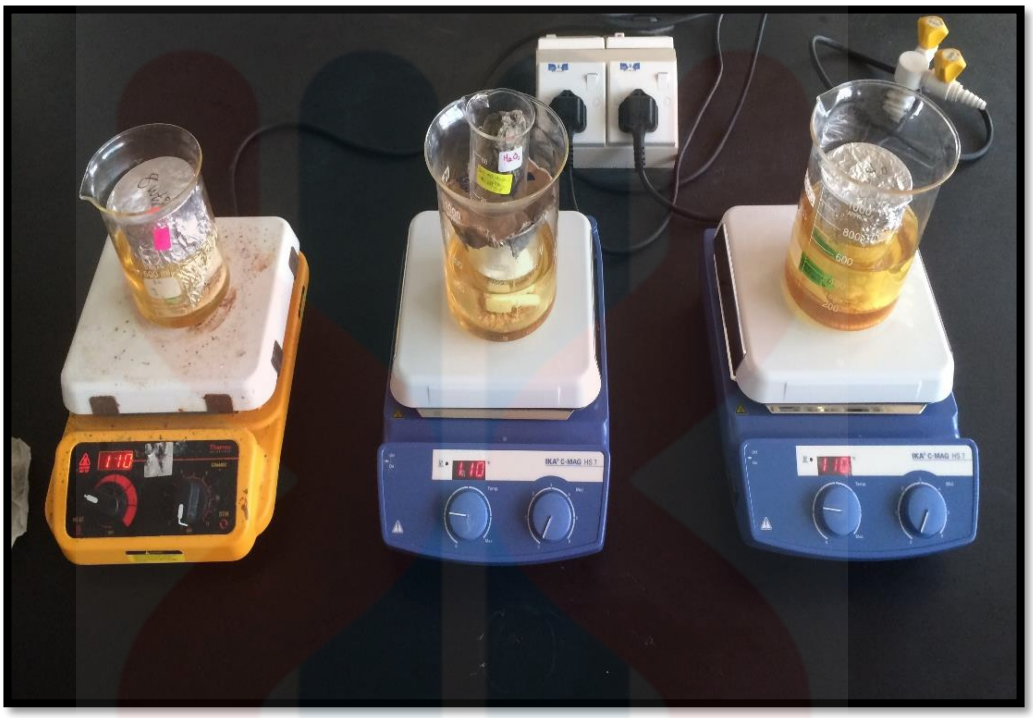

Figure 3.6: 2 wt %, 5 wt% and 8 wt% of regenerated celluloses production

Figure 3.7: Regenerated cellulose (NCCs) obtained after freeze dry

3.2 Characterization method

The characterizations of regenerated celluloses or nanocellulose (NCCs) were examined and carried out by using 4 main machines. X-ray diffraction (XRD), Fourier transform infrared analysis (FTIR) and field emission-scanning electron microscopy (FESEM) characterized the structural change and also the morphology of the nanocellulose (NCCs). Besides, thermogravimetric analysis (TGA) characterized the thermal properties of the NCCs that was obtained.

3.2.1 X-ray Diffraction (XRD)

X-ray diffractometer (XRD) was used to study the crystallinity of NCCs from mahang wood (*Macaranga spp.*). It was equipped with CuKα radiation (λ=1.5418 Å) in the 2θ range of 5˚ to 60˚, in step mode with a step of 0.01˚ and a rate of 1˚/ min^{-1}. The operating voltage was 40 kV and the current was 40 mA (Tan et al., 2015). The crystallinity index value is computed according to Segal's method as stated at equation 3.1:

$$\text{CrI}\ (\%) = \frac{(I_{002} - I_{am})}{I_{002}} \tag{3.1}$$

where I_{002} was the peak intensity corresponded to crystalline and I_{am} was the peak intensity of the amorphous fraction (Li et al., 2010).

Scherrer equation as stated at equation 3.2 also was used in this study to measure the crystallite size of each sample that perpendicular to (002) planes, w (nm):

$$w = \frac{K\lambda}{\beta \cos\theta} \tag{3.2}$$

where θ was the diffraction angle, K= 0.94 (correction factor), λ = 0.154 nm and β (FWHM) were the corrected angular width in radians at half maximum intensity of the (002) peak (Tan et al., 2015).

3.2.2 Fourier transform infrared analysis (FTIR)

FTIR was used to study the different functional groups of extracted NCCs by obtained the FTIR spectra. The sample was pounded to made a thin pellet that was the mixture of approximately 5 mg of particles samples and 95 mg of finely ground KBr. Then, the spectra were viewed by using FTIR machine. The spectra produced was transmittance mode between wave numbers of 4000 cm^{-1} and 500 cm^{-1} (Lamaming et al., 2015).

3.2.3 Field emission-scanning electron microscopy (FESEM)

FESEM was used to study the surface morphology of the extracted NCCs, 2 wt % regenerated celluloses (Tan et al., 2015). The morphology of the sample was examined by JEOL (JSM-7800 F) field emission scanning electron microscopy at an acceleration voltage of 5 kV. The sample was sputtered coated with gold using sputter coater.

3.2.4 Thermogravimetric analysis (TGA)

The dynamic thermogravimetric measurement was performing by thermogravimetric analysis (TGA) to measure the mass change of the materials with the increase of temperature. The samples of approximately 7 mg of each sample were heated from room temperature to 500˚C at a heating rate of 10 K min^{-1}. In order to prevent premature thermoxidative degradation, all measurements were performed under a nitrogen atmosphere with a gas flow of 20 cm^3 min^{-1} (measured at 289 K and 101.3 kPa) (Tan et al., 2015).

RESEARCH FLOWCHART

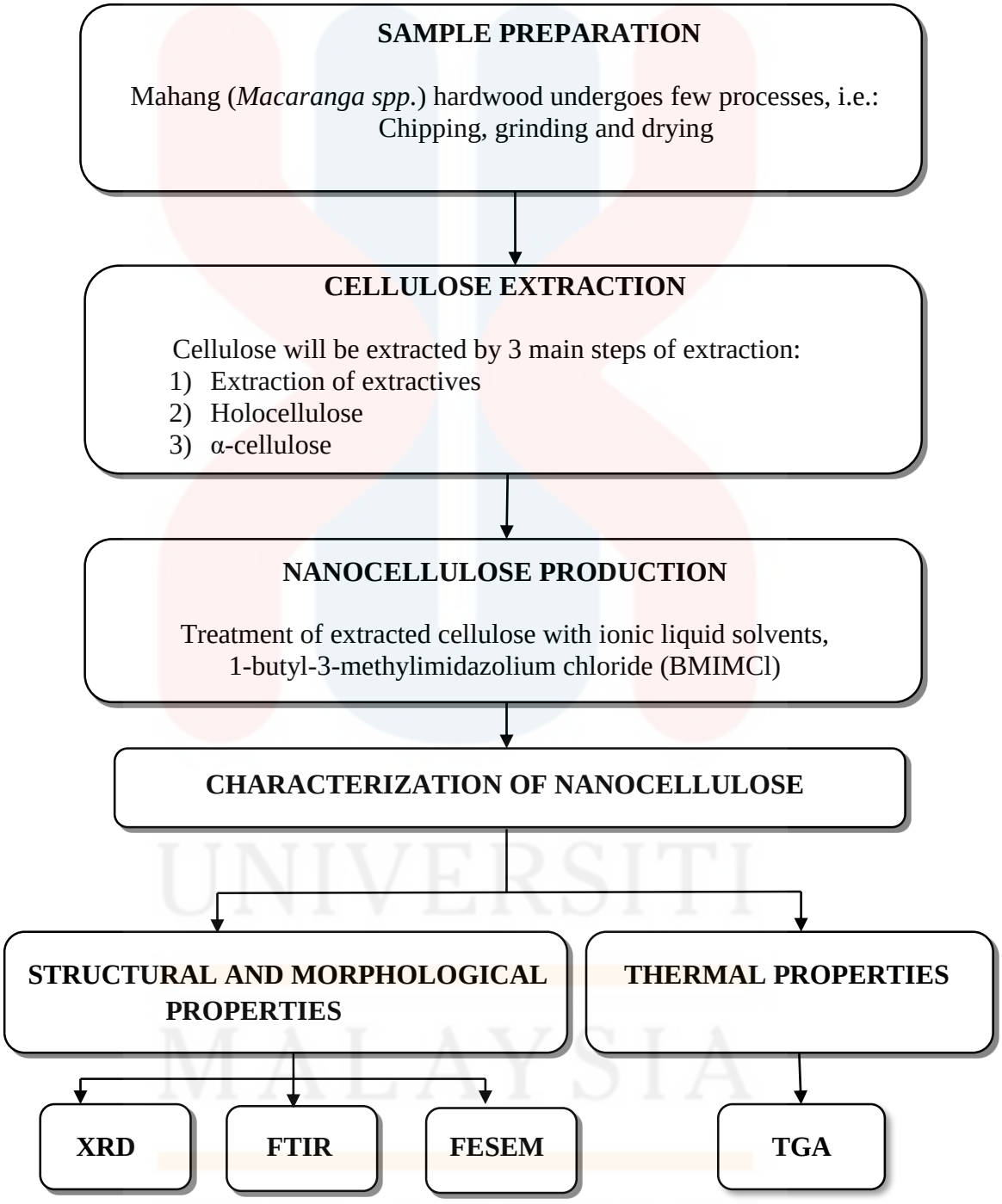

Figure 3.8: Research flowchart.

CHAPTER 4

RESULTS AND DISCUSSION

The characterizations of all samples that are the cellulose pure (MCC), alpha cellulose (extracted cellulose) and regenerated celluloses (2 wt %, 5 wt % and 8 wt%) were analyzed by X-ray diffraction (XRD), Fourier transform infrared analysis (FTIR), field emission-scanning electron microscopy (FESEM), and thermogravimetric analysis (TGA) analysis. Cellulose pure (MCC) was the standardize cellulose and alpha cellulose was the cellulose that obtained by the extraction process. Besides, three ionic liquid treated samples were prepared from the extracted cellulose with different amount weight percentages (2 wt %, 5 wt % and 8 wt%). XRD, FTIR, and FESEM were used to characterize the structural change and morphology of the samples respectively. Meanwhile, TGA was used to study the thermal properties of the samples that were obtained.

4.1 XRD analysis

The crystallinity of samples was characterized by XRD. Figure 4.1 showed all of the XRD patterns with ordered structure of crystalline and amorphous region. Three characteristics peaks of cellulose pure (MMC) showed at 2θ = 14.9°, 16.5°, and 22.6° which corresponded to the crystallographic plane of crystals (110), (110), and (002) respectively. Alpha cellulose, which was the cellulose that has been extracted from mahang wood showed a slightly different pattern which it was more amorphous and less sharp peak at 2θ = 19.75° compared to the cellulose pure (MCC) that has a sharper peak at 2θ = 22.6° and more crystalline region. These differences were probably due to the

disrupted of ordered structure of the crystalline region of the alpha cellulose by the extraction process (Zhu et al., 2006).

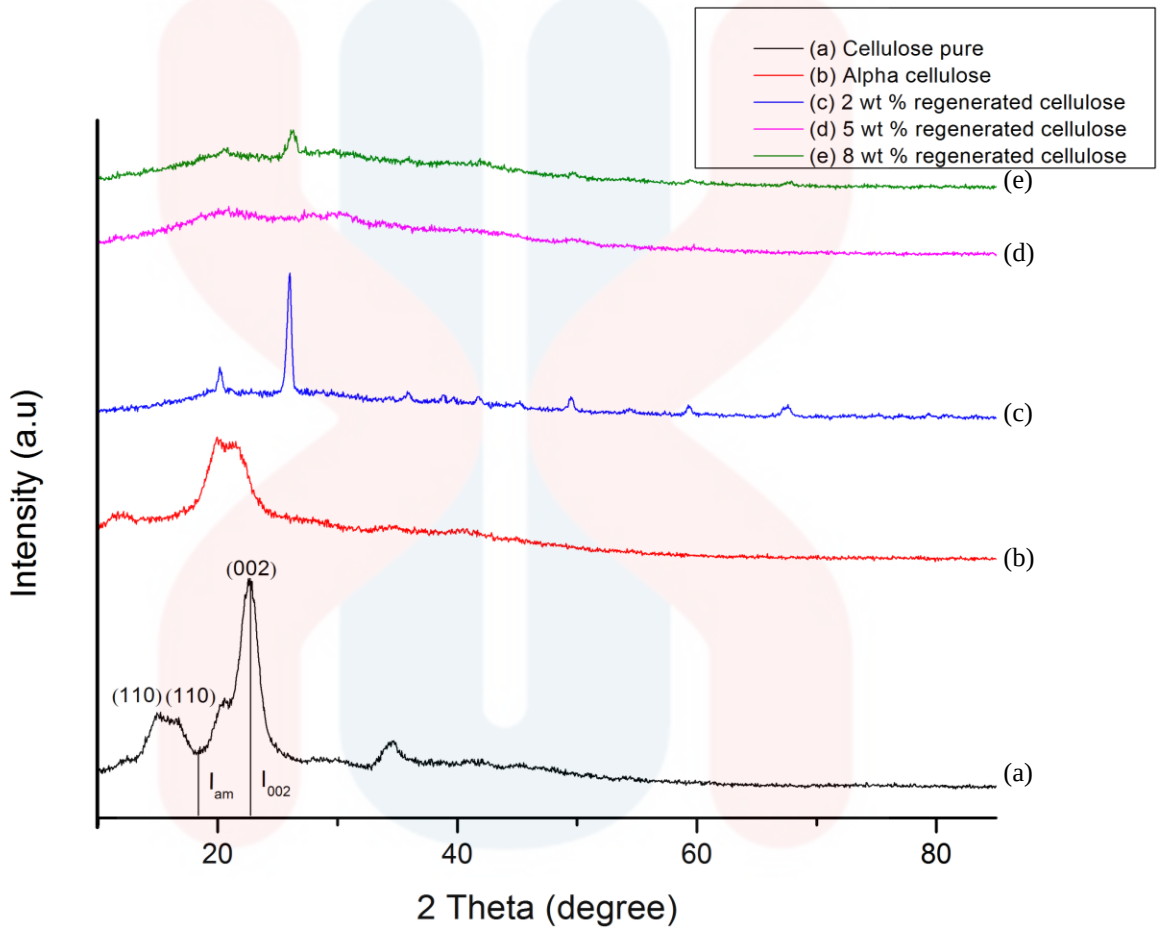

Figure 4.1 XRD pattern of cellulose pure MMC (a), alpha cellulose (b) and regenerated cellulose treated with ionic liquid at 2 wt% (c), 5 wt % (d) and 8 wt % (e).

Moreover, Figure 4.2 showed 2 wt % of regenerated cellulose that has high crystalline cellulose pattern with the occurrence of a most intense and sharper peak (002) at 2θ = 26.10°. The high amount of intense and sharper peak pattern 2 wt % regenerated cellulose was very correlate to the real properties and characteristics of nanocellulose (NCCs) which was high crystallinity. Besides, 2 wt % regenerated cellulose pattern indicated that the regenerated cellulose obtained with a high amount of IL have more crystalline region because IL had selectively removed the amorphous region pattern.

Other than that, by comparing between 2 wt %, 5 wt % and 8 wt % regenerated celluloses, 2 wt % illustrated high intense peak with high crystallinity compared to 5 wt % and 8 wt %. Besides that, this high crystallinity of 2 wt % of regenerated cellulose may due to the highest amount of ionic liquid treated ratio compared to 5 wt % and 8 wt %. Plus, 5 wt % and 8 wt % of regenerated celluloses showed the amorphous pattern after IL pretreatment because the peak (101) and (002) became broader and disappeared. The amorphous patterns indicated that during the treatment with IL process, the regenerated cellulose bonding were unable to break apart the inter and intra chain of hydrogen bonding in the cellulose fibrils (Li et al., 2010).

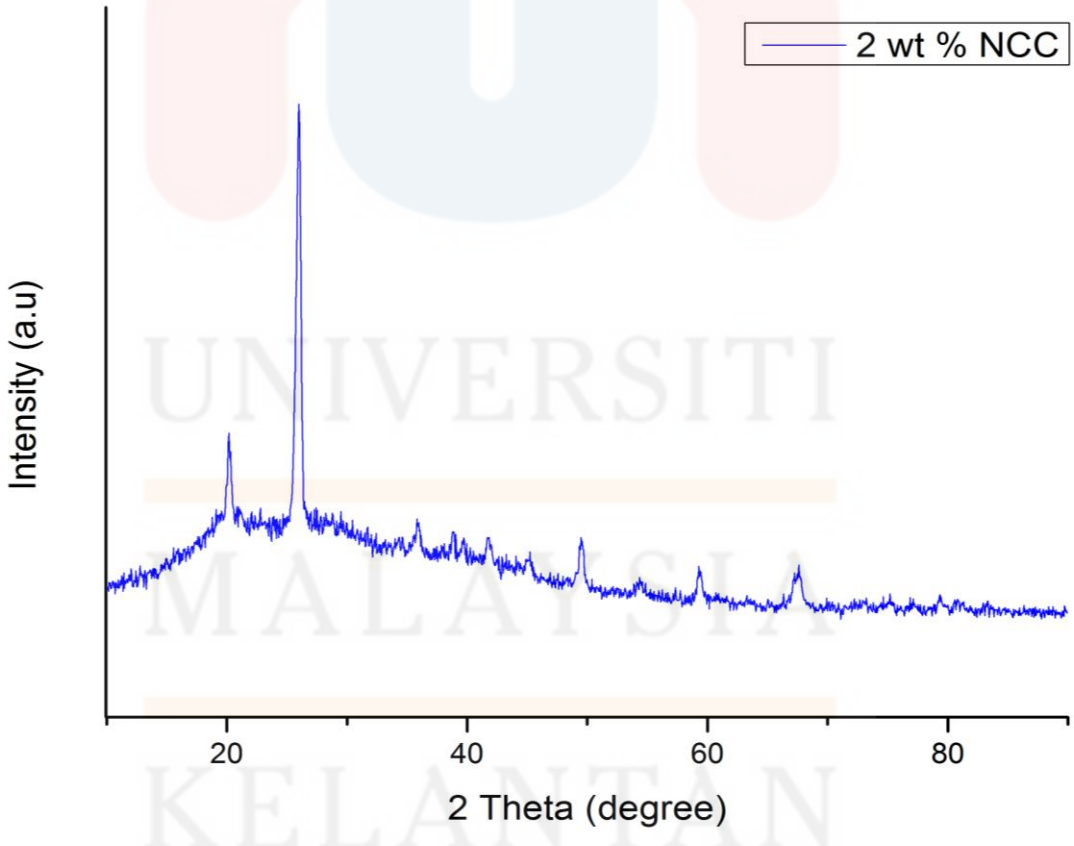

Figure 4.2 XRD pattern of 2 wt % regenerated celluloses, NCCs.

Based on the areas under the diffraction curves, the application of the surface method for calculating the crystallinity index (Crl) for each pattern was calculated by using the Segal's method as stated in Equation 4.1:

$$\mathrm{Crl} = \frac{\mathrm{I_{002}} - \mathrm{I_{am}}}{\mathrm{I_{002}}} \tag{4.1}$$

The intensity value of the 002 crystalline peak (I_{002}) and the height of minimum (I_{am}) were used in the Crl calculation (Segal's method).

On the other hand, the crystallite size of each sample that perpendicular to (002) planes, *w* (nm), was calculated by using the Scherrer Equation to measure the crystallite size (*see* Equation 4.2).

$$w = \frac{\mathrm{K\lambda}}{\beta \cos \theta} \tag{4.2}$$

In Equation 4.2, θ was the value of diffraction angle, K= 0.94 (correction factor), λ = 0.154 nm and β (FWHM) was the corrected angular width in radians at half maximum intensity of the (002) peak. The value of θ and β also must be converted to radian first before obtained the calculations of crystallite size.

The calculations of crystallinity index (%) and crystallite size (nm) have tabulated in Table 4.1. As shown in Table 4.1, the crystallinity index (Crl) and crystallite size of cellulose pure (MCC) are higher than the alpha cellulose. This indicates alpha cellulose has a lower amount of crystallinity compared to cellulose pure (MCC). Besides, all of the regenerated celluloses has an estimated 5 – 45 % lower crystallinity index compared to cellulose pure (MCC). Plus, 2 wt % of regenerated cellulose shows

higher crystallinity index which is 74.76 % compared to 5 wt % and 8 wt % of regenerated cellulose which is 56.33% and 35.90% respectively.

The crystallite size of 2 wt % of regenerated cellulose also is the largest size which is 15.22 nm compared to 5 wt % and 8 wt % of regenerated celluloses which are only 0.40 nm and 0.32 nm respectively. Hence, this smaller in crystallite sizes was due to the incomplete growing of crystallites after regeneration (Gao et al., 2011).Plus, the improved crystallinity index and crystallite size can attribute to the progressive reduction and removal of the amorphous parts of cellulose as the amount of IL increased (Tan et al., 2015).

Table 4.1 The crystallinity index (Crl) and crystallite size of MMC and regenerated celluloses prepared with different weight ratio (2 wt %, 5 wt % and 8 wt%).

Sample	Crystallinity Index (%)	Crystallite size (nm)
(a) Cellulose pure MMC	78.10	4.61
(b) Alpha cellulose	59.74	2.34
(c) 2 wt % NCCs	74.76	15.22
(d) 5 wt % NCCs	56.33	0.40
(e) 8 wt % NCCs	35.90	0.32

4.2 FTIR analysis

In order to gain more insights into the effects of ILs pretreatments, the characterizations on the chemical and structural characteristics of all samples includes cellulose pure (MCC), alpha cellulose, 2 wt %, 5 wt % and 8 wt % of regenerated cellulose are essential. Hence, FTIR spectra showed in Figure 4.3 illustrated that all spectra samples were almost identical which indicated no changes in the functional group. The absorption bands at ~663, ~895, ~1053, ~1430, ~1637, ~2983 and ~3331 cm^{-1} in the spectrum of cellulose pure (MCC) are associated with the alpha cellulose and also the regenerated celluloses that have been treated with different wt %.

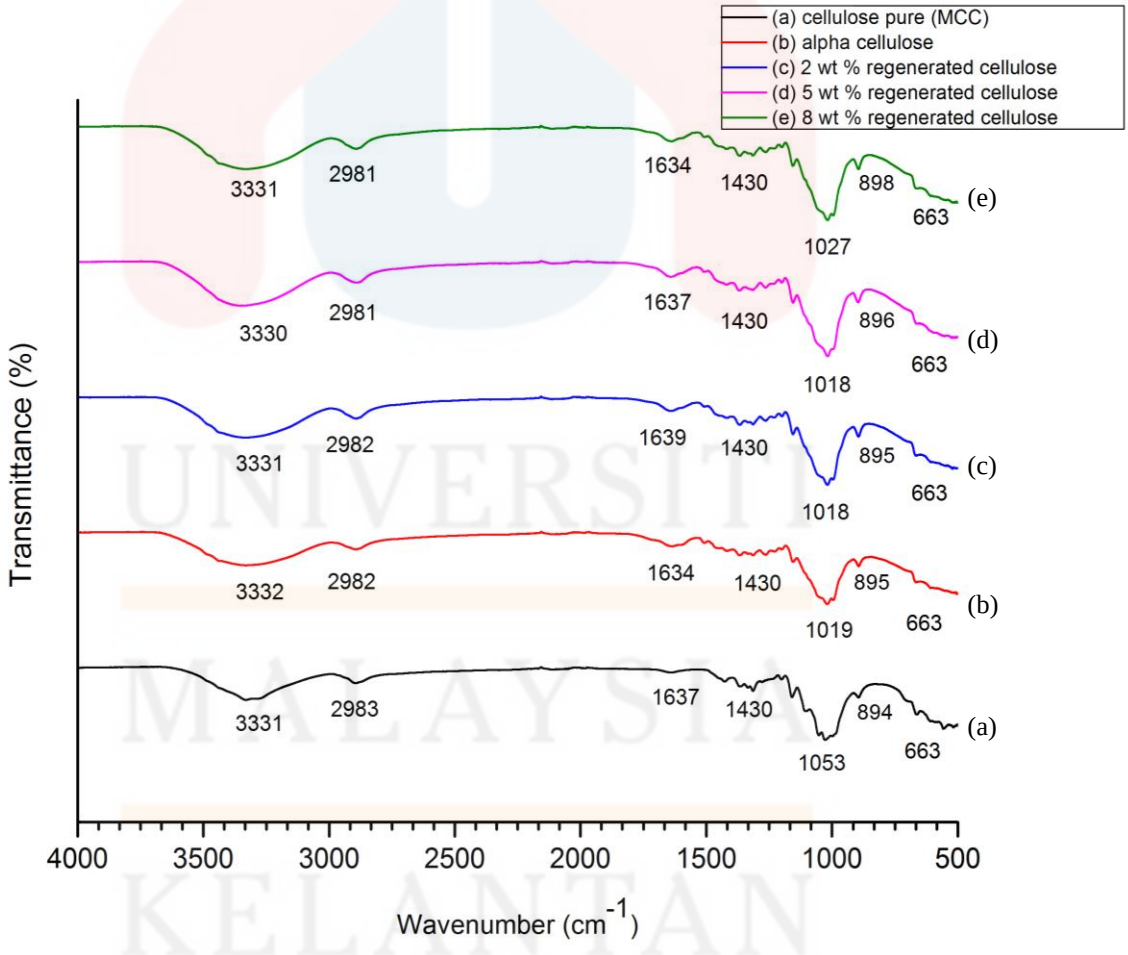

Figure 4.3 FTIR Spectra of Cellulose pure MMC (a), alpha cellulose (b) and regenerated cellulose treated with Ionic Liquid (IL) at 2 wt% (c), 5 wt % (d) and 8 wt % (e).

Moreover, all of the samples showed a broad of bands in the region 3600 to 3200 cm^{-1} that indicate to the characteristics of hydrogen bond (O-H) stretching vibrations. O-H stretching vibrations defined as the bending vibrations of water molecules. Hence, we can assume that at the regions 3600 to 3200 cm^{-1}, the presence of water is abundance. Plus, the spectrum of cellulose pure (MMC) is sharpest in the spectrum region (3600 to 3200 cm^{-1}) of O-H stretching vibrations compared to other samples which are broader in spectrum region due to the presence of water during the process of extraction and treatment with IL.

Besides, sp^3 C-H stretching vibrations and O-H bending of absorbed water have risen to the peak at ~2983 cm^{-1} and ~1637 cm^{-1} respectively by all of the samples. C-H is considered as the asymmetric in cellulose-rich material and the bending of CH_3 and methoxy ($-OCH_3$). A sharp peak was detected at ~1430 cm^{-1} of all samples spectrum that ascribed to the intermolecular hydrogen attraction at the C_6 group. Furthermore, this sharp peak was stronger for crystalline cellulose while relatively weak in amorphous cellulose.

Other than that, all of the samples spectrums have a sharp peak observed at ~1053 cm^{-1} spectrum that indicated to the stretching vibrations of C-O-C pyranose ring (antisymmetric in phase ring) of cellulose molecules. Besides, the sharp peak regions corresponded to the C-O stretching vibrations in cellulose, hemicellulose, and lignin and this clearly explains the lignocellulosic structure of mahang powder.

Meanwhile, all of the samples showed a broad of spectrum in the region ~895 cm^{-1} that correlated to the higher amount of disordered cellulosic structure. This disorder amount of cellulosic structure is very likely caused by the deformation vibration of β-glycosidic linkages and hydrogen bond rearrangement (Lan et al., 2011). The spectra lie

in the range of 1100 cm^{-1} and 600 cm^{-1} indicated the vibration of wagging, deformation and twisting modes of anhydro-glucopyranose. Furthermore, the absence of peaks of BMIMCL in the spectra also determined the complete removal of IL during the washing process. The group frequency of absorption bands of cellulosic samples has been tabulated in table 4.2 (Tan et al., 2015).

Table 4.2: Group frequency of absorption bands of cellulosic samples

Group frequency, wavenumber, cm^{-1}	Origin	Assignment
~895	C-H	C-H deformation vibration in cellulose
~1035	C-O	C-O stretching vibration in cellulose
~1430	O-H	Intermolecular hydrogen attraction at the C_6 group
~1637	O-H	O-H of water absorbed from cellulose
~2983	C-H	C-H stretching in cellulose-rich material
3600 - 3200	O-H	Free and hydrogen-bonded OH stretching

4.3 FESEM Analysis

FESEM analysis was done in order to provide topographical and elemental information of regenerated cellulose. The structural morphology of 2 wt % regenerated cellulose was examined at high and low magnification. As seen in the image at high magnification (Figure 4.4(a)), 2 wt % of regenerated cellulose appeared as rough structure fiber. Close-up an image of regenerated cellulose fiber as showed in Figure 4.4 (a) clearly indicates the structure was composed of very rough surface layer of fiber.

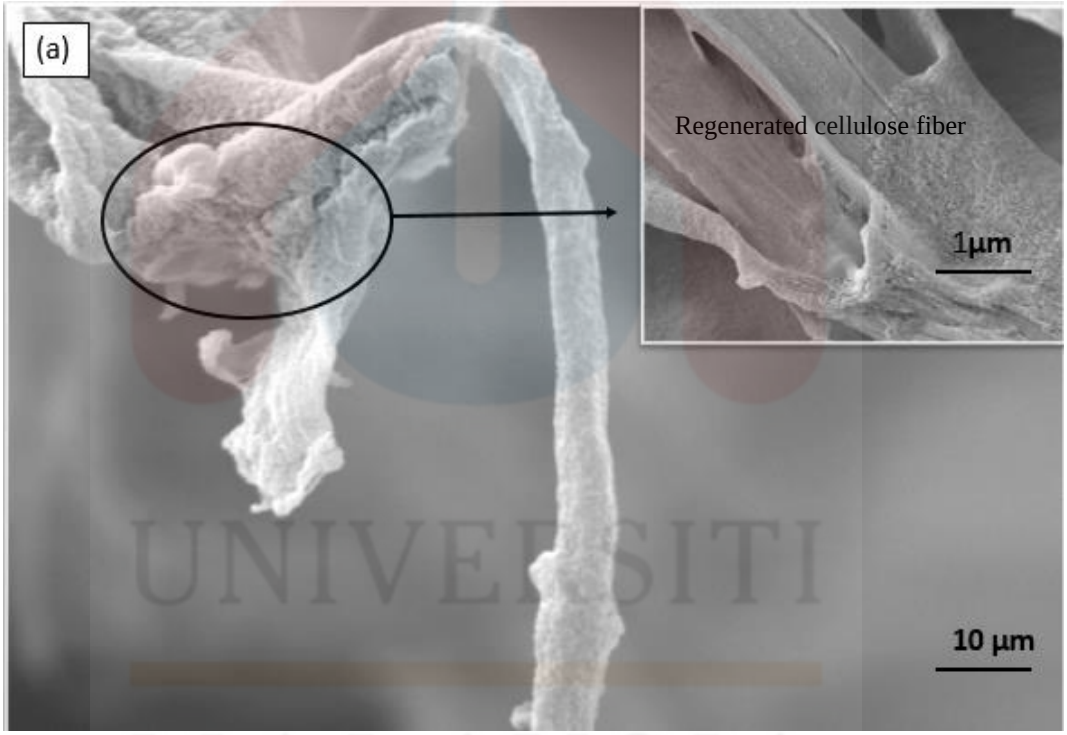

Figure 4.4 (a): Structure and appearance of 2 wt % regenerated cellulose fiber by FESEM at high magnification (×15000).

Besides that, at low magnification level (Figure 4.4 (b) and (c)) the images showed irregular shapes with close up of image micrograph that showed conglomerate and also very rough surface structures of 2 wt % regenerated cellulose fibers.

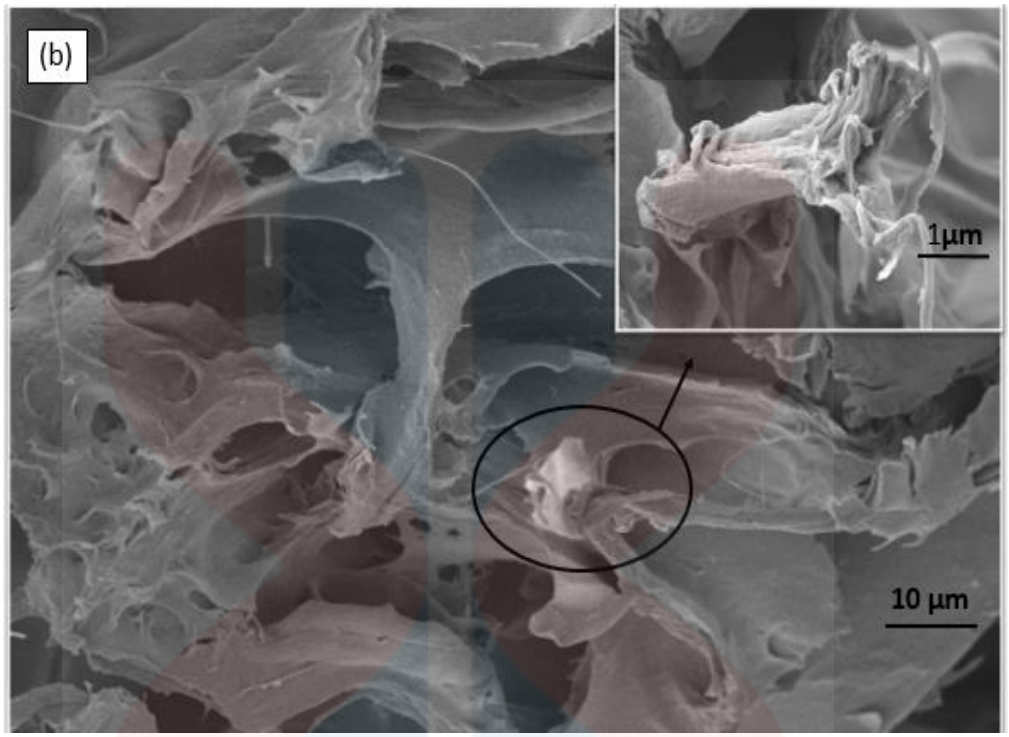

Figure 4.4 (b): Structure and appearance of 2 wt % regenerated cellulose fiber by FESEM at low magnification (×800).

.

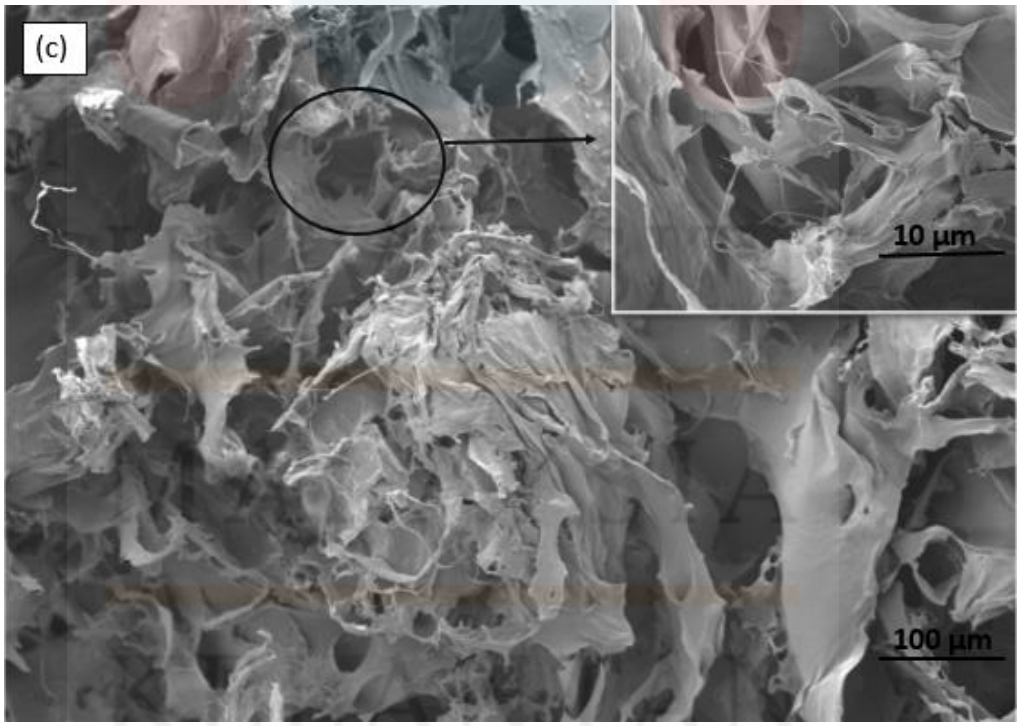

Figure 4.4 (c): Structure and appearance of 2 wt % regenerated cellulose fiber by FESEM at low magnifications (×500)

Apart from that, at very low magnification level as shown in Figure 4.4 (d) the image of regenerated cellulose fibers also appeared as very rough structure. This appearance of the rough structure may due to the micro size of cellulose fibers that tend to separate from a bundle of fibrils after regeneration with ionic liquid (Tan et al., 2015). To sum up, all of the image that micrographs by FESEM showed the rough and conglomerate structure of 2 wt % regenerated cellulose fibers.

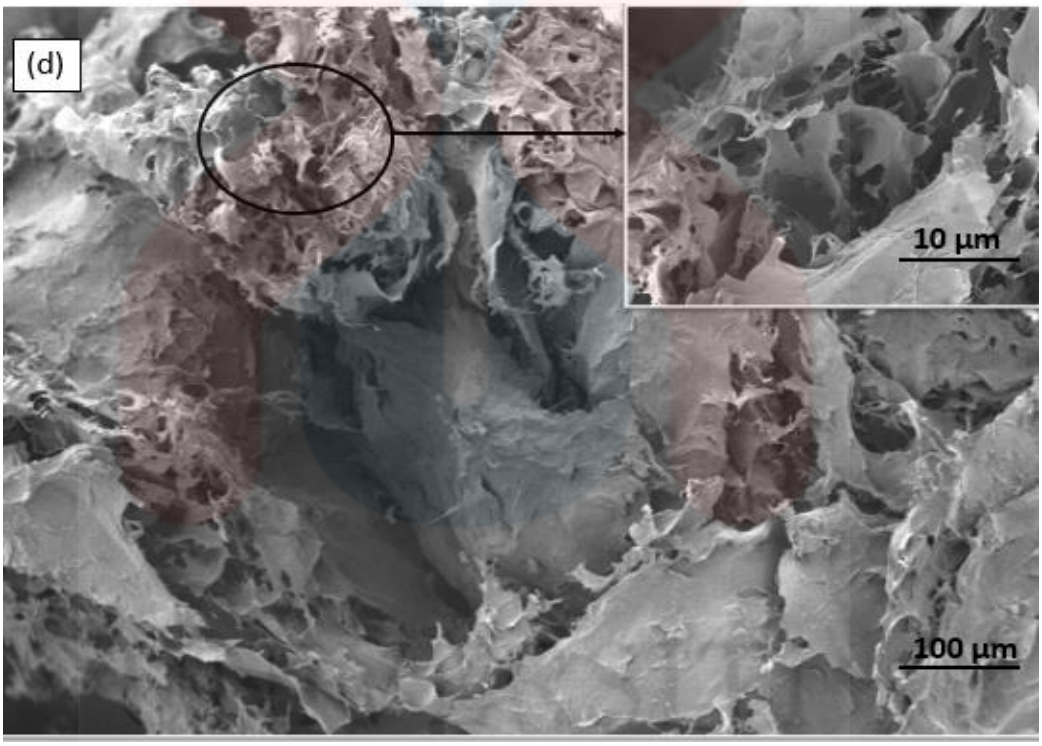

Figure 4.4 (d): Structure and appearance of 2 wt % regenerated cellulose fiber by FESEM at very low magnification (×60).

4.4 TGA Analysis

Thermogravimetric (TG) and differential thermogravimetric (DTG) analysis of lignocellulosic biomass of mahang powder provide the information on the thermal decomposition profiles of respective components that can be used to follow the physiochemical changes that occurred during the IL pretreatments process. Figure 4.5 (a) and (b) showed the thermogravimetric (TG) and its derivatives (DTG) of cellulose Pure (MMC), alpha cellulose and also regenerated cellulose, NCCs (2 wt %, 5 wt % and 8 wt %) respectively.

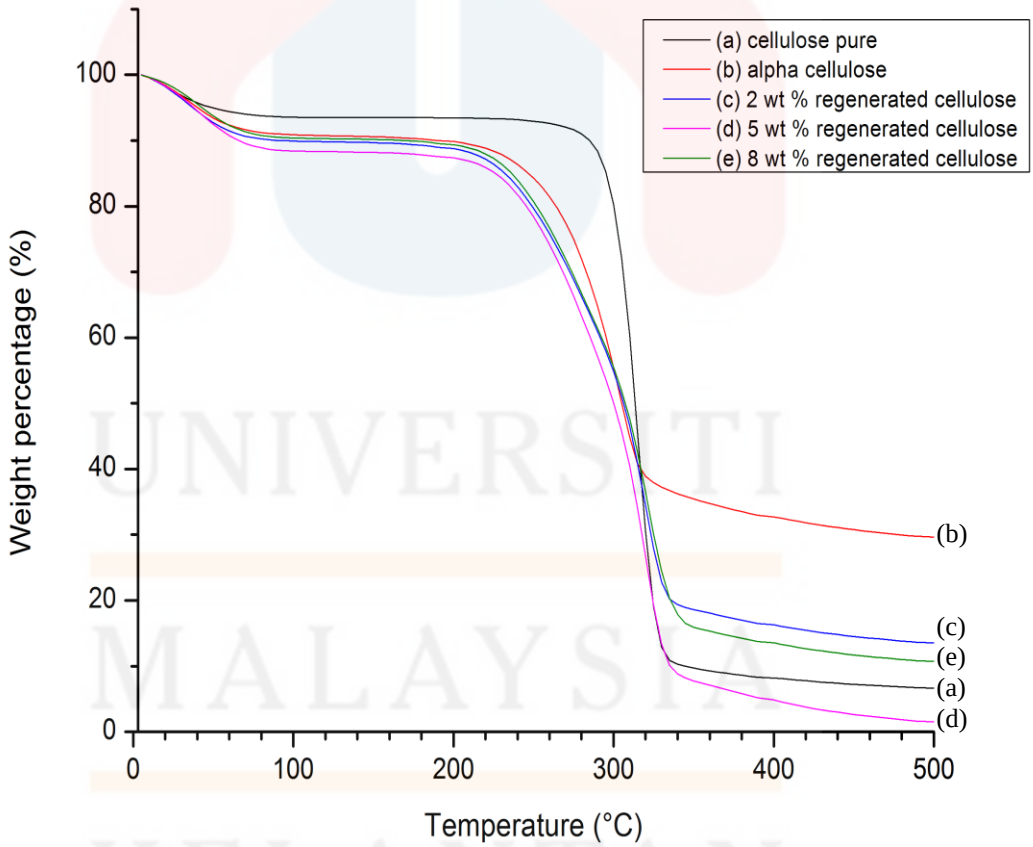

Figure 4.5 (a): TG curves for cellulose pure MMC (a), alpha cellulose (b) and 2 wt% (c), 5 wt % (d) and 8 wt % (e) of regenerated cellulose.

At the temperature below 100 °C, all of the samples had an initial small amount of weight loss that indicates to the evaporation of water loosely bound to the surfaces of cellulose**.** At all curves of the samples, a single remarkable decomposition associated with progressive weight loss was observed.

At relatively narrow range of temperature (310 °C - 380°C), the decomposition of cellulose pure (MMC) took place and indicates only one-step pyrolysis process by the DTG curves. In addition, the decomposition of alpha cellulose took place at the temperature (250 °C -370°C) and also illustrated one step pyrolysis process.

The decomposition of regenerated cellulose within a wider range of weight percentage with two distinct pyrolysis process that well separated in close proximity as revealed by the curves of DTG (Tan et al., 2015). The first pyrolysis of regenerated cellulose occurred from 220 °C to 280 °C with the T_{max} peak at 240 °C that attributes to the decomposition of highly accessible regions, while the second pyrolysis had greater dominance over the first pyrolysis, ranging from 280 °C to 350 °C with T_{max} at 325 °C that represented to the breakdown of the crystal interior.

The value of T_{max} derived from TGA data represents the temperature at which the maximum decomposition occurs. Hence, T_{max} is used to evaluate the impact of IL pretreatment on the thermal stability of samples.

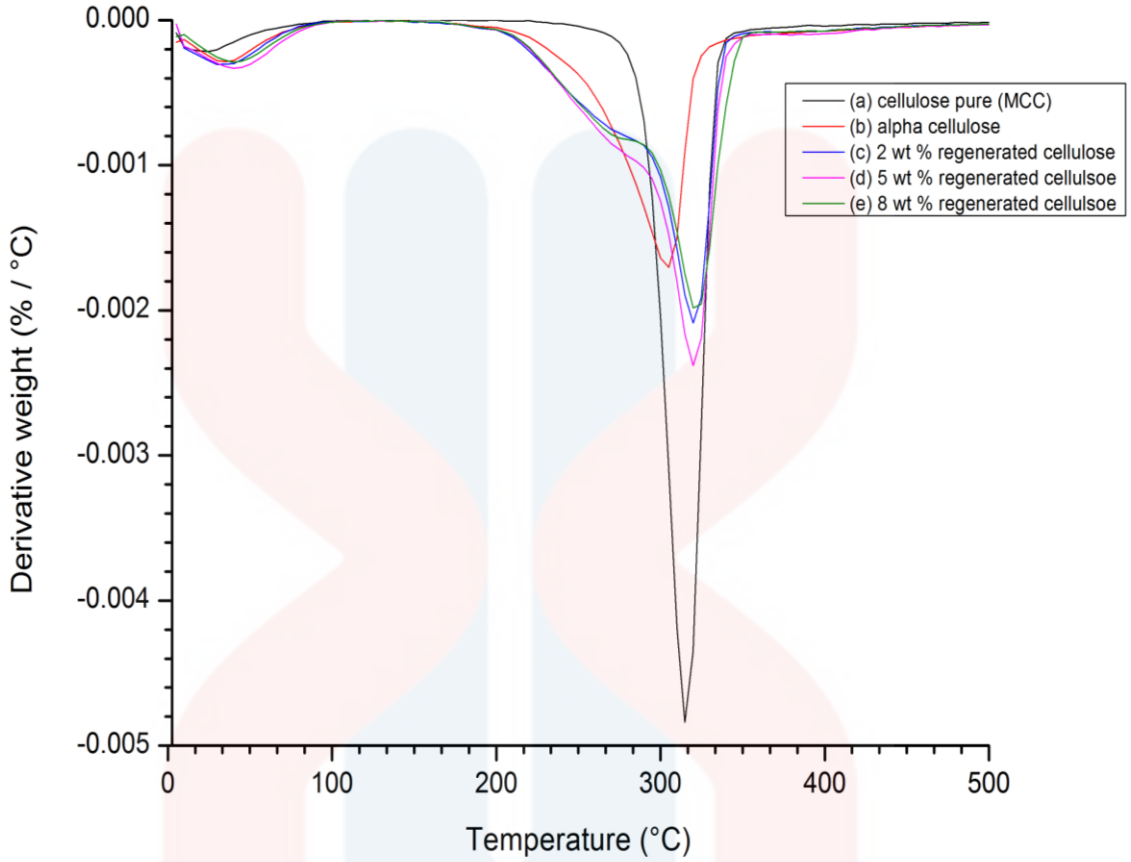

Figure 4.5 (b): DTG curves for cellulose pure MMC (a), alpha cellulose (b) and 2 wt% (c), 5 wt % (d) and 8 wt % (e) of regenerated cellulose.

Therefore, it can be deduced that one-step pyrolysis process occurred for the MCC and two-step pyrolysis process occurred for regenerated celluloses, NCCs. This difference in thermal degradation was probably due to the degree of crystallinity. Besides, the two peaks that observed in two-step pyrolysis process could be due to the presence of both crystalline and amorphous components in the regenerated cellulose. In general, it is easier to breakdown the amorphous region at a lower temperature followed by weight loss due to the crystalline components, which decompose at high temperature. Moreover, the reduction in molecular weight of regenerated cellulose also caused the decomposition temperature of regenerated cellulose (2 wt %, 5 wt % and 8 wt %) lower

than MCC (cellulose pure and alpha cellulose).

The decreasing trend of decomposition temperature concludes that the thermal stability of regenerated cellulose was lower than MCC. Besides, this reduction in thermal stability could be due to several factors such as the thermal stability that reduced for regenerated cellulose due to the high surface area fiber dimensions compared to macroscopic cellulose which increases the heat exposure and also the delignification occurring at higher pretreatments temperature may also contribute to lower the thermal stability (Tan et al., 2015).

.

CHAPTER 5

CONCLUSION AND RECOMMENDATIONS

Regenerated cellulose, were successfully prepared from the extracted alpha cellulose (MCC) using an environmentally friendly and green chemistry approach that is by using the ionic liquid (BMIMCl). XRD, FTIR, FESEM, and TGA analysis showed different patterns of regenerated cellulose compared to MCC.

From the XRD results, 2 wt % of regenerated cellulose had higher crystalline cellulose pattern with the occurrence of a most intense and sharper peak with higher crystallinity index and crystallite size compared to 5 wt % and 8 wt % regenerated celluloses. The peaks of 5 wt % and 8 wt % of regenerated cellulose were broad and also low in terms of crystallinity index and crystallite size that may due to the incomplete growing after regeneration. Hence, this concludes that only 2 wt % of regenerated cellulose, that obtained with the highest amount of ionic liquid percentage was the one of the regenerated cellulose that very correlated to the real properties and characteristics of nanocellulose (NCCs).

Based on the FTIR spectroscopy, the spectrum of all samples showed a similar pattern to each other. Besides, the slight difference in terms of the peak of absorption band that represents the O-H band, C-H band, C-O stretching vibration, intermolecular hydrogen attraction at the C_6 group and others also obtained from the further analysis with FTIR. Cellulose pure sample shows a small different pattern at the absorption band ~3331 cm^{-1} compared to alpha cellulose and also the regenerated cellulose that may due to the present of water during the process of extraction and treatment with BMIMCl.

Apart from that. FESEM results illustrate that all of the images that micrographs at a high and low magnification of 2 wt % of regenerated cellulose fibers appeared as rough and conglomerate surface textures. Last but not least, TGA results concludes that one-step pyrolysis process occurred for the MCC and two-step pyrolysis process occurred for regenerated celluloses, NCCs. This differences in thermal degradation were probably due to the degree of crystallinity.

To sum up, it can be concluded that one of the regenerated cellulose, 2 wt % was the most successful treatment with BMIMCl because it has high crystallinity that suits to the real properties of the nanocellulose compared to 5 wt % and 8 wt %. Hence, the regenerated celluloses have been obtained in this study and the characterizations also have been analyzed by XRD, FTIR, FESEM and TGA. Hence, from all of the characterizations of regenerated celluloses, only 2 wt % regenerated celluloses can be correlate to the real properties and characteristics of nanocellulose (NCCs). This desired property also can be correlate to the highest amount of ionic liquid used. Thus, the purpose of this study was achieved.

For the recommendations for this study, in order to get better properties of nanocellulose (NCCs), the combinations of chemical and physical treatments are one of the proposed methods that can enhance specific properties and characterizations. The physical treatments such as homogenization might useful for improving the production process of nanocellulose. Last but not least, to further the analysis of NCCs, transmission electron microscopy (TEM) might be useful to observe features such as the crystal structure and the structure of dislocations and grain boundaries. This is because TEM is the very powerful tool in material science that shone thoroughly the high energy beam of an electron through the sample that can provide useful information.

REFERENCES

Ang, A., Ashaari, Z., Bakar, E. S., & Sahri, M. H. (2009). Modern Applied Science. *Enhancing the Properties of Mahang (Macaranga Spp.) Wood through Acrylic Treatment in Combination with Crosslinker*, 3(11), 2–10.

Ang, A. F., Zaidon, A., Bakar, E. S., Mohd Hamami, S., Anwar, U. M. K., & Jawaid, M. (2014). Possibility of improving the properties of mahang wood (Macaranga sp.) through phenolic compreg technique. *Sains Malaysiana*, 43(2), 219–225.

Bee, S., Hamid, A., Lee, H. V, Hamid, S. B. A., & Zain, S. K. (2015). Conversion of Lignocellulosic Biomass to Nanocellulose: Structure and Chemical Process. *Conversion of Lignocellulosic Biomass to Nanocellulose*, 1–21.

Chen.Hz. (2014). Biotechnology of Lignocellulose: Theory and Practice. *Chemical Composition and Structure of Natural Lignocellulose*, 25-72.

Dufresne, A. (2013). Nanocellulose: A new ageless bionanomaterial. *Materials Today*, 16(6), 220–227.

Frone, A. N., Panaitescu, D. M., & Donescu, D. (2011). Some aspects concerning the isolation of cellulose micro and nano fibers. *UPB Scientific Bulletin, Series B: Chemistry and Materials Science*, 73(2), 133–152.

Gao, Q., Shen, X., & Lu, X. (2011). Regenerated bacterial cellulose fibers prepared by the NMMO·H_2O process. *Carbohydrate Polymers*, 83(3), 1253–1256.

Gardner, K., & Blackwell, J. (1974). The structure of native cellulose. *Biopolymers*, 13(10), 1975–2001.

Granström, M., & Kilpeläinen, P. I. (2009). *Cellulose Derivatives: Synthesis, Properties and Applications*. *Department of Chemistry* (Vol. PhD), 120.

Habibi, Y., Lucia, L. a, & Rojas, O. J. (2009). Cellulose Nanocrystals : Chemistry, Self-Assembly, and Applications. *Chemical Reviews*, *d*, 3479–3500.

Hwa, H., & Wang, C. (2009). Cellulose and pulp. *Forest and Forest Plants*, *II*, 344.

Jung, B., & Theato, P. (2012). Chemical Strategies for the Synthesis of Protein – Polymer Conjugates. *Advances in Polymer Science*, (May 2012), 1–34.

Klemm, D., Kramer, F., Moritz, S., Lindstrom, T., Ankerfors, M., Gray, D., & Dorris, A. (2011). Nanocelluloses: A new family of nature-based materials. *Angewandte Chemie - International Edition*, 50(24), 5438–5466.

Kopania, E., Wietecha, J., & Ciechańska, D. (2012). Studies on isolation of cellulose fibres from waste plant biomass. *Fibres and Textiles in Eastern Europe*, 96(6 B), 167–172.

Laine, C. (2005). Structures of hemicelluloses and pectins in wood wood pulp. *Department of Chemical Technology, Doctor of*, 63.

Lamaming, J., Hashim, R., Sulaiman, O., Leh, C. P., Sugimoto, T., & Nordin, N. A. (2015). Cellulose nanocrystals isolated from oil palm trunk. *Carbohydrate Polymers*, 127, 202–208.

Lan, W., Liu, C., Yue, F., Sun, R., & Kennedy, J. F. (2011). Ultrasound-assisted dissolution of cellulose in ionic liquid. *Carbohydrate Polymers*, 86(2), 672–677.

Lee, K. Y., Aitomki, Y., Berglund, L. A., Oksman, K., & Bismarck, A. (2014). On the use of nanocellulose as reinforcement in polymer matrix composites. *Composites Science and Technology*, 105, 15–27.

Li, C., Knierim, B., Manisseri, C., Arora, R., Scheller, H. V., Auer, M., Singh, S. (2010). Comparison of dilute acid and ionic liquid pretreatment of switchgrass: Biomass recalcitrance, delignification, and enzymatic saccharification. *Bioresource Technology*, 101(13), 4900–4906.

Ma, N., Liu, D., Liu, Y., & Sui, G. (2015). Extraction and Characterization of Nanocellulose from Xanthoceras Sorbifolia Husks. *International Journal of Nanoscience and Nanoengineering*, 2(6), 43–50.

Mat Zain, N. F. (2014). Preparation and Characterization of Cellulose and Nanocellulose From Pomelo (Citrus grandis) Albedo. *Journal of Nutrition & Food Sciences*, 05(01), 10–13.

Mohammad, B., Islam, T., Alam, M. M., Torino, P., Patrucco, A., & Mon-, A. (2014). Preparation of Nanocellulose : A Review. *Preparation of Nanocellulose*, 1(5), 17–23.

Morais, J. P. S., Rosa, M. D. F., De Souza Filho, M. D. S. M., Nascimento, L. D., Do Nascimento, D. M., & Cassales, A. R. (2013). Extraction and characterization of nanocellulose structures from raw cotton linter. *Carbohydrate Polymers*, 91(1), 229–235.

Moran, J. I., Alvarez, V. A., Cyras, V. P., & Vazquez, A. (2008). Extraction of cellulose and preparation of nanocellulose from sisal fibers. *Cellulose*, 15(1), 149–159.

Noor Azrieda, A. R., Razali, A. K., Rahim, S., & Izran, K. (2012). Physical and mechanical properties of portland cement-bonded flakeboards fabricated from macaranga gigantea and neolamarckia cadamba. *Pertanika Journal of Tropical Agricultural Science*, 35(4), 783–792.

Oksman, K., Etang, J. A., Mathew, A. P., & Jonoobi, M. (2011). Cellulose nanowhiskers separated from a bio-residue from wood bioethanol production. *Biomass and Bioenergy*, 35(1), 146–152.

Pandey, K. K. (1999). A study of chemical structure of soft and harwood and wood polymers by FTIR spectrscopy. *Journal of Applied Polymer Science*, 71(May),

1969–1975.

Soni, B., Hassan, E. B., & Mahmoud, B. (2015). Chemical isolation and characterization of different cellulose nanofibers from cotton stalks. *Carbohydrate Polymers*, 134, 581–589.

Tan, H. T., Lee, K. T., & Mohamed, A. R. (2011). Pretreatment of lignocellulosic palm biomass using a solvent-ionic liquid [BMIM]Cl for glucose recovery: An optimisation study using response surface methodology. *Carbohydrate Polymers*, 83(4), 1862–1868.

Tan, X. Y., Abd Hamid, S. B., & Lai, C. W. (2015). Preparation of high crystallinity cellulose nanocrystals (CNCs) by ionic liquid solvolysis. *Biomass and Bioenergy*, 81, 584–591.

Zakaria, R., Fadzly, N., Rosely, N., Mansor, M., & Zakaria, M. Y. (2008). The distribution of macaranga, Genus (Family Euphorbiaceae) in Penang Island, Peninsular Malaysia. *Journal of Bioscience*, 19(2), 91–99.

Zhu, S., Wu, Y., Chen, Q., Yu, Z., Wang, C., Jin, S., Wu, G. (2006). Dissolution of cellulose with ionic liquids and its application: a mini-review. *Green Chemistry*, 8(4), 325.

APPENDICES

A 1: Mahang powder

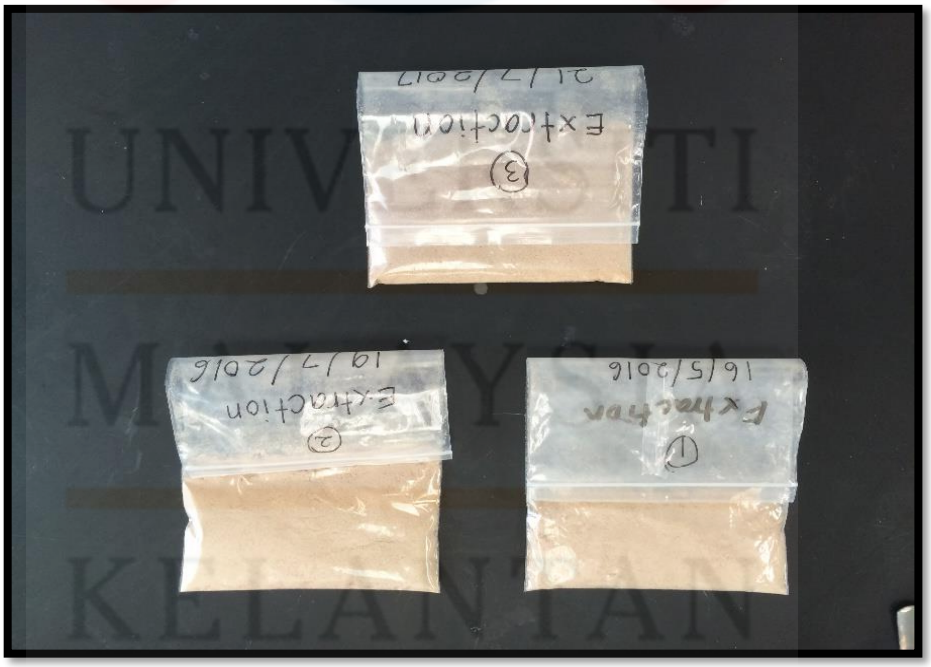

A 2: Extraction samples after oven dry

A 3: Holocellulose sample after oven dry

A 4: Alpha cellulose obtained after oven dry

A 5: Completed regenerated celluloses production

A 6: Separation process of ionic liquid